

LAUNCH TRAFFIC MODEL FOR SPACE DEBRIS EVOLUTION BASED ON HISTORICAL DATA AND ECONOMIC FORECASTING METHODS

Wiebke Retagne, Elisa Boccolari, and Camilla Colombo

Politecnico di Milano, 20156 Milano, Italy, Email: {wiebke.retagne, elisa.boccolari, camilla.colombo}@polimi.it

ABSTRACT

When modeling the evolution of the space debris environment, the launch traffic plays a crucial role. Even minor changes in simulated traffic have a substantial influence on parameters like the collision risk and the total number of fragments. Most of the launch traffic patterns used in current space debris models are based on historical data extrapolation, implemented by simply repeating the launches of the recent years. While this provides a good starting point, it does not accurately capture the emerging trends in space activities. With commercial spaceflight on the rise, the trend is going towards placing satellites in orbit distributed missions composed by small satellites and large constellations. These recent changes need to be captured in a launch traffic model. This research is part of the GREEN SPECIES project, funded by the European Research Council on the “Robust control of the space debris population to define optimal policies and an economic revenue model for sustainable development of space activities”. This work aims at developing a highly adaptable and accurate launch traffic model by combining the study of historical data with economic and financial forecasting methods such as the Autoregressive Integrated Moving Average (ARIMA), the Prophet model and Long Short-Term Memory (LSTM). This will allow a better adaption of the modeling of the debris environment and the design of mitigation action to the actual evolution of space activities and its impact in the orbital space.

To accurately compare and discuss existing space debris evolutionary models and their limitations inputs such as the launch traffic model needs to be clearly defined. As a starting point a comprehensive overview of the existing launch traffic models, and their assumptions will be given. This survey will be useful to assess how varying assumptions affect predictions and the accuracy of space debris risk assessments. Following the literature study, a new model is developed to address the identified gaps. As a novelty, economic forecasting methods are used to predict the development of space activities and particularly the launch traffic. In particular, three time-series forecasting methods will be studied: Autoregressive Integrated Moving Average (ARIMA), the Prophet model and Long Short-Term Memory (LSTM). The ARIMA approach is commonly used to predict stock prices and trends or to predict economic development such as infla-

tion rates. The LSTM has also shown good results in predicting economic growth rates and is well suited to deal with time-series data. Both of these methods can provide a way of capturing the underlying patterns and are suitable for long-term forecasting. The different launch traffic models obtained with the two approaches are produced and compared with the literature launch models. The effect of the predicted launch activity on the future environment is then studied with the COMETA debris evolutionary model that allows to project the objects population into the future under the effect of objects’ sources and sinks.

Keywords: Space Debris Modelling; Time-Series Forecasting; Launch Traffic; Machine Learning in Space; Long term debris evolution; Population modelling.

1. INTRODUCTION

The evolution of the space debris environment is very sensitive to its input parameters. One of these parameters is the launch traffic model, used to predict the future launches each year. Depending on the number of launches, parameters such as the collision risk increase drastically. A sensitivity analysis on the launch traffic has been performed in [1]. For simplicity, a lot of launch models repeat the launch traffic. This approach is applied in several models, such as EVOLVE [2], DAMAGE [3], LEGEND [4], and MEDEE [5], where an eight-year launch cycle is typically used. In this work time series methods are employed instead. These are often used for financial forecasting and predict the future development of a parameter based on the historical data. An overview of these methods can be found in [6]. Furthermore, not only the number of launches influences the space debris environment. The position of these objects in orbit play a major role in the future evolution of space debris. In this work the total number of objects launched each year is determined using time-series methods. The ARIMA model [7], the Prophet model [8] and the LSTM model [9] are used to forecast the future trend of launches. The best parameters for each of these models are determined through the Mean-Squared-Error (MSE) between actual historical data and the forecast. The next 100 years are forecasted. Then, the results are compared to two litera-

ture models.

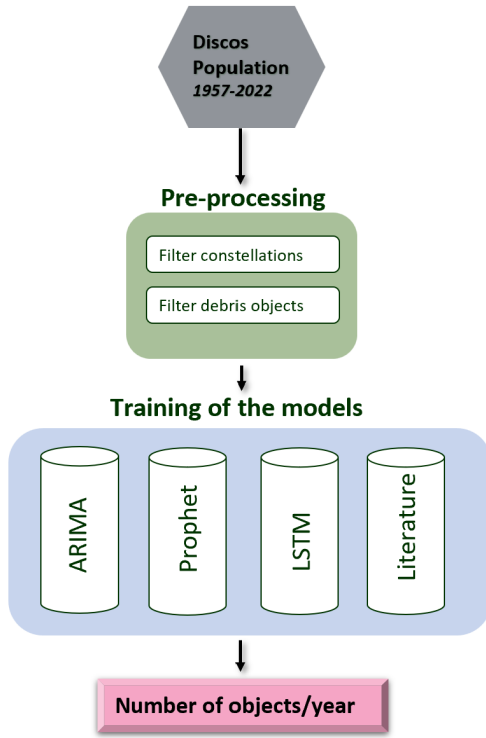


Figure 1. To determine the number of objects launched each year different models are trained on pre-processed historical data.

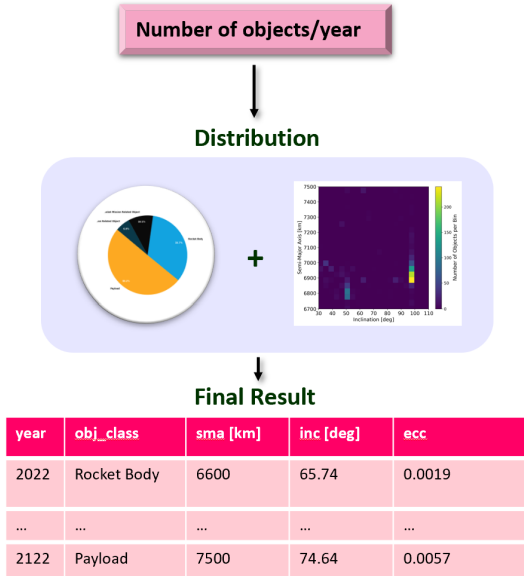


Figure 2. The orbital parameters and the category of the objects are determined through a distribution build on historical data

After pre-processing of the historical data, sourced from the ESA DISCOS database [10], the total number of objects is determined with different models, as can be seen in Fig. 1. Then, their position is assigned through sampling from a distribution built on historical data in 3 dimensions: The semi-major axis, the inclination and the eccentricity for the different object categories. The final result can be seen in Fig. 2. Finally, the simulated launch traffic is used as an input in COMETA, a debris evolutionary model to determine the effect of the launches on the space debris population as a whole.

1.1. The history of launches

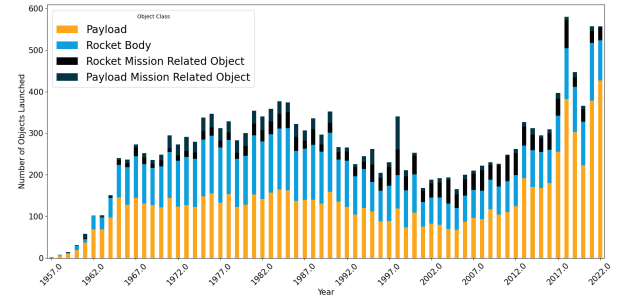


Figure 3. The historical launch data divided into the object categories.

With the first satellite launch of Sputnik 1 in 1957 the Space Race between the Soviet Union and the United States (U.S.) commenced. During 1962 to 1969 there is a noticeable increase in launches corresponding to the height of the Space Race. In between 1969-1972 the Apollo program was at its peak, with the U.S sending numerous missions to the moon. With the introduction of the reusable space shuttle in 1981 the number of launches increased slightly. After 1989 there is a drop in the number of launches, which may be due to the reduced focus on space after the end of the Cold War, the collapse of the Soviet Union in 1991 and the Challenger disaster in 1986. Between 2000 and 2010 the public interest in space decreased drastically. The early 2000 recession had a major impact also on the space economy. This further demonstrates the link between economic strength and the number of launches. After 2010 there is a significant rise, probably related to the increased availability of commercial space launchers. This is also reflected in the increased number of payloads being launched. Commercial launchers are able to launch numerous missions at once, with the focus of private companies being on payloads that generate data they can sell.

2. THE NUMBER OF OBJECTS LAUNCHED EACH YEAR

As a first step the number of objects launched each year will be modeled. This describes solely the non-

constellation objects, since constellations follow a very different more deterministic pattern compared to non-constellation objects. To develop a forecast three main methods are investigated. The Autoregressive Integrated Moving Average (ARIMA) (3), the Prophet model (4) and the Long Short-Term Memory (LSTM) (5). The historical data is sourced from the ESA DISCOS database [10]. There is data available from 1957-2022 (see Fig. 3). In a pre-processing, the constellation objects and debris objects are filtered out.

3. ARIMA MODEL

The ARIMA model [7] is a time series forecasting method that combines Autoregression (AR), Integrated (I) and Moving Average (MA) components. The AR part models the relationship between an observation and its so called lagged (previous) observation, thereby capturing temporal dependencies. The parameter p describes the number of lags used as predictors. The differencing transforms the data to remove trends or seasonality, making it stationary. The parameter d describes the minimum number of differences needed to make the time-series stationary. The MA models short-term fluctuations by considering error terms of previous observations. The parameter q determines how many error terms are to be included in the model. The key part of an accurate ARIMA model is to fine-tune these parameters according to the historical data. To better understand the historical launch data the time-series is decomposed into its components: the trend, the seasonality and the residuals in Fig. 4.

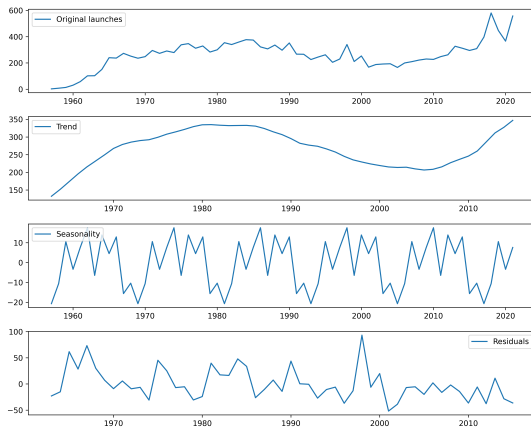


Figure 4. The launch data decomposed into its trend, seasonality and the residuals.

A general upwards trend and a seasonal pattern can be observed. The seasonality could be due to external factors such as fiscal deadlines, weather conditions or optimal orbital windows for launches. The residuals describe any part not covered by the trend or seasonality. There are some pronounced spikes in the residuals, which might correspond to unexpected events such as the drop

in launches after 1990. Furthermore, a Dickey-Fuller test [11] is implemented to check for stationary in the time-series. The Dickey-Fuller test checks for the presence of a unit root, which indicates non-stationarity. If a time-series is stationary its statistical properties do not depend on the time at which they were observed. The p-value was determined to be $p > 0.05$, hence the time-series is non stationary. Since the ARIMA model assumes stationarity, differencing has to be applied to make it stationary.

3.1. Tuning of the model

The parameters (p, q, d) must be carefully chosen. There are several approaches to tune the parameters. In this work, a training and test dataset are defined based on the historical launch data. This allows to determine the accuracy of the forecast based on the MSE between these. Then the best MSE is determined with a grid search approach to find the best combination of (p, q, d) . Furthermore, the training period has to be set. This includes the decision on whether or not to use all historical launch data or only include the most recent years. Three different starting points are investigated: 1957, 1980 and 2005. In all cases the data is split into 66% train data and 34% test data. Then for each of these starting points the best parameters (p, q, d) are determined using a grid search which tests different combinations of the parameters and determines the best combination based on the MSE. In Fig. 5 the result of the best parameters in the training for the different starting points 1957 (green X), 1980 (yellow diamond) and 2005 (red star) and the historical data (blue dots) are plotted against each other. The best MSE is achieved by using the dataset starting in 1980.

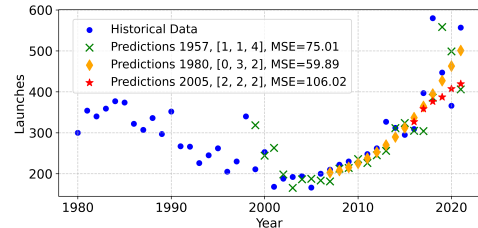


Figure 5. The different starting points to determine the best ARIMA parameters.

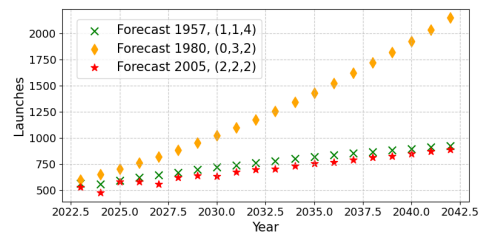


Figure 6. The forecast using different ARIMA parameters.

To determine the correct parameters not only the comparison to historical data is important. Also the development of the forecast in the future needs to be judged. In Fig. 6 the forecast for the future 20 years is plotted. Here, the nature of the different parameter curves is seen more clearly. When using data starting from 2005 a linear approximation is modeled. Data from 1980 yields a steeply growing curve. While the data from 1980 delivered the best MSE, it is not realistic that the launches keep on growing with no bound. Instead, when using the entire dataset from 1957 a realistic steadily growing curve is achieved. For the rest of this work ARIMA refers to the model trained on data from 1957 with the parameters $(p, q, d) = (1, 1, 4)$.

4. PROPHET MODEL

The Prophet model [8] is a forecast model developed specifically for ease of use. It uses a decomposable time series model with three main components: trend $g(t)$, seasonality $s(t)$ and holidays $h(t)$, as seen in Eq. 1.

$$y(t) = g(t) + s(t) + h(t) + \alpha. \quad (1)$$

The α represents the residual item, which follows a normal distribution. Each item is fitted separately and the combination of them yields the final result. Prophet is robust to outliers, meaning that if there are unusual spikes in the launches due to one-time events or unforeseen circumstances, the model can still make reliable predictions. The Prophet model works with either a linear or a logistic growth trend and can model seasonal effects and special events. It is well suited to sparse data such as the historical data on launches and does not require complex manual tuning like the ARIMA model. Since the model is made up of three parts, there are three main hyperparameters in the Prophet model. The *changepoint_prior_scale*, which controls how sensitive the model is to changes in the trend. The *seasonality_prior_scale* which controls the strength of the seasonality effect and the *holidays_prior_scale*, which adjusts for holidays or special events, which can be added as external regressors. In the fitting process, the Prophet model automatically determines the best values for all parameters to minimize the error between the predicted and the actual data. For this, Prophet uses a Bayesian approach in a Markov Chain Monte Carlo [12] method to minimise the loss function. After the model is fitted, Prophet generates forecasted values including uncertainty intervals. Here, Prophet uses Monte Carlo simulations to generate a distribution of the possible future outcomes. Furthermore, cross-validation can be used to assess the model performance. Here, different subsets of data is used to see how well the model handles unseen data. When using Prophet with the launch traffic data the parameters presented in Tab. 1 are used.

Table 1. The parameters used for the Prophet model.

Parameter	Value
<i>changepoint_prior_scale</i>	0.5
<i>seasonality_prior_scale</i>	0.1
<i>holidays_prior_scale</i>	0.1

5. LSTM MODEL

In comparison to the ARIMA or the Prophet model the Long-Short-Term Memory (LSTM) model is much more complicated. Instead of a statistical method or a fitting process it uses machine learning to predict the future values. In particular it is a type of Recurrent Neural Network (RNN) designed to learn from sequential data. It maintains the memory of previous information. The core components are:

- Cell state: Acts as a memory, carrying relevant information across time steps.
- Forget gate: Decides what information to discard from the cell state.
- Input gate: Determines what new information to add.
- Output gate: Controls the output and what part of the cell state to expose.

For the implementation of the LSTM model the python library tensorflow is used. This library provides easily implementable and reliable algorithms.

5.1. Tuning of the model

When building an LSTM model several hyperparameters are important for the final result of the forecast. For the training of the model the dataset was split into 77% training and 23% data. The best results were achieved when using data starting from 1980 and ranging to 2021. The sequence length describes the number of time steps in each input sequence fed to the LSTM. For this model 5 consecutive years were used as sequence length. In this work a custom loss function is defined. The loss function describes the difference between the actual value and the predicted value. In the ARIMA model the MSE was used as a simple guideline to determine the best parameters. For the training of the LSTM model a more complicated custom loss-function is implemented. The custom loss function is designed to incorporate both the squared error loss and penalties for predictions that are outside certain bounds. The penalty is based on the average yearly change in launches, which includes both increases and decreases. Let the following definitions hold: Let $L(t)$ denote the number of launches in year t . The change in

launches, $\Delta L(t)$, is calculated as the difference between consecutive years in Eq. 2.

$$\Delta L(t) = L(t) - L(t-1). \quad (2)$$

The average decline in launches, $\overline{\Delta L^-}$, and the average increase, $\overline{\Delta L^+}$, are computed in Eq. 3 and Eq. 4.

$$\overline{\Delta L^-} = \text{mean}(\Delta L(t) \mid \Delta L(t) < 0), \quad (3)$$

$$\overline{\Delta L^+} = \text{mean}(\Delta L(t) \mid \Delta L(t) > 0). \quad (4)$$

Let $L(T)$ denote the last known launch count in the dataset. A custom loss function is defined to penalise predictions that deviate significantly from expected trends. The loss function is designed to incorporate penalties for predictions that fall below a lower bound or exceed an upper bound in Eq. 5.

$$\text{penalty_lower} = L(T) + 1.8 \cdot \overline{\Delta L^-}, \quad (5)$$

$$\text{penalty_upper} = L(T) + 1.0 \cdot \overline{\Delta L^+}. \quad (6)$$

The custom loss function, $\mathcal{L}(y, \hat{y})$, with y, \hat{y} the actual value and its prediction, is then formulated in Eq. 7.

$$\mathcal{L}(y, \hat{y}) = \text{MSE}(y, \hat{y}) + \text{penalty_low}(\hat{y}) + \text{penalty_high}(\hat{y}), \quad (7)$$

where MSE is the mean squared error, and the penalty terms in Eq. 8 and Eq. 9.

$$\text{penalty_low}(\hat{y}) = \exp(\max(\text{penalty_lower} - \hat{y}, -5)) - 1, \quad (8)$$

$$\text{penalty_high}(\hat{y}) = 2 \cdot (\max(0, \hat{y} - \text{penalty_upper}))^2. \quad (9)$$

The low penalty is applied when the predicted value is lower than the threshold based on the last known value and the average decline in launches. Similarly the high penalty is applied when the predicted values exceed a threshold based on the last known value and the average increase in launches. The low penalty grows exponentially, ensuring that the model does not predict unusually low values. The high penalty grows quadratically, avoiding large overestimation. Together with the squared error the final loss function ensures that the model predicts values close to the actual ones and does not generate any extreme values in either direction.

6. LITERATURE MODELS

The launch traffic model most commonly used in space debris evolution studies involves repeating the launch data from the past years. This approach is applied in several models, such as EVOLVE [2], DAMAGE [3], LEGEND [4], and MEDEE [5], where an eight-year launch cycle is typically used. For the purpose of this paper, a five-year cycle (2020–2024) has been selected. This decision accounts for the significant increase in launches in recent years, particularly from 2021 onward.

Using a longer cycle that includes earlier years with lower launch rates would not accurately represent the current trend. Additionally, only individual payloads have been considered, with large satellite constellations—such as Starlink—excluded. This exclusion drastically reduces the total number of launches per year, bringing the peak down from over 2,500 satellites in 2023 to approximately 600.

Another approach is to extrapolate the data from previous years. In the work of Velerda [13] the number of launches per year is estimated using Gompertz logistic curves, defined in Eq. 10.

$$L(t) = \left[a \exp(-e^{-b-c(t-t_0)}) + d \right], \quad (10)$$

where L is the number of launches in the year t and t_0 is a reference year. The other parameters are obtained by a fit to the data ranging between $t_0 = 2005 - 2021$. The parameter a describes the saturation point, which is chosen based on a low and high rate scenario before fitting the curve. This way, the effect of future variations of the total number of launches is assessed. To assess the accuracy of the here described time-series models the same approach is applied to the data used for the previously described models. This leads to the parameters described in Tab. 2.

Table 2. Coefficients for low and high launch rates.

Coefficient	Low Rate	High Rate
a	1100.000000	1500.000000
b	1.164903	1.219842
c	0.110938	0.088033
d	100.000000	100.000000

7. COMPARISON OF DIFFERENT LAUNCH MODELS

To discuss the validity of the different launch models all of the trained models are used to forecast the next 100 years. The result can be seen in Fig. 7. Plotted are the historical data (blue dots), the ARIMA model (green X), the Prophet model (purple dots), Velerda low rate (yellow diamond), Velerda high rate (red star), LSTM (black triangle) and the cyclic repetition (pink pentagon). Most notably, all models except the Prophet one show a saturation point. The Prophet model keeps on continuously linearly growing. In the year of 2122 the final number of launches for the different models is displayed in Tab. 3.

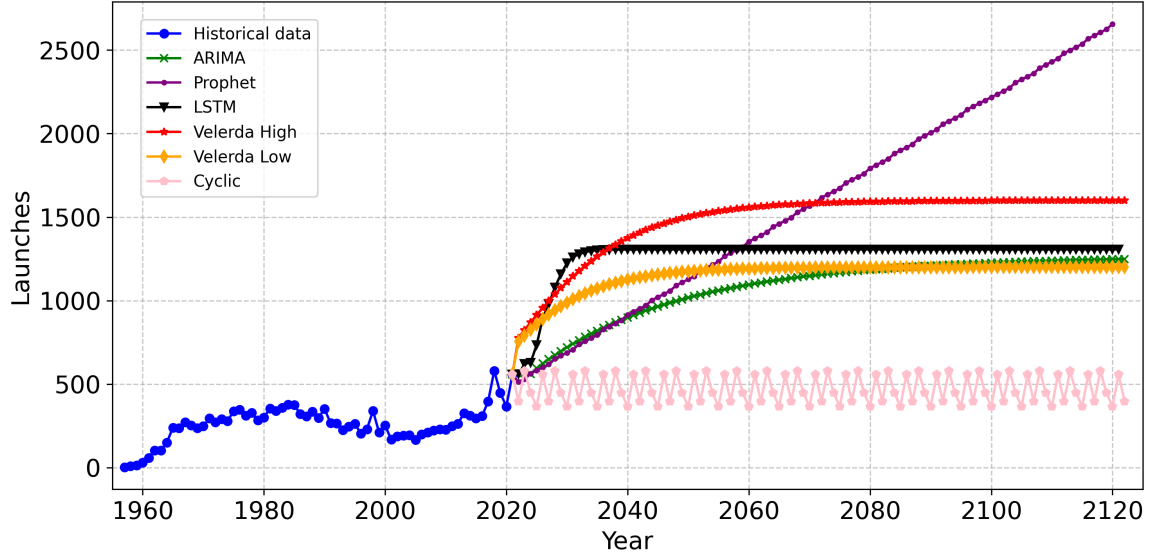


Figure 7. The historical data and the different launch models forecasted for a time span of 100 years.

Table 3. The final number of launches for the different launch models in the year of 2122

Model	Final number of launches
ARIMA	1248
Prophet	2656
LSTM	1200
Velerda High	1600
Velerda Low	1306
Cyclic	397

The final number of launches is similar for the ARIMA, LSTM, and Velerda [13] low rate. The Prophet model predicts almost double this value. The cyclic repetition severely underestimates the number of launches in compared to the other models. The ARIMA model shows a steady upward trend, Velerda [13] models are trending upwards at a moderate rate. The Prophet shows more aggressive growth. Notably only after the 50 years the Prophet exceeds the other models. While most of them reach a saturation the Prophet one keeps growing. The cyclic repetitions is the only model that captures downward trends over time. This constant upward trend (with a saturation) might not be representative of the reality, since historical events and economic growth can strongly impact the number of space launches. For this reason in future work the launch model should not only be based on the historic data but also consider adjunct influences such as economic investment in space.

8. EVOLUTION OF THE SPACE DEBRIS ENVIRONMENT

The launch models derived in this work are simulated using COMETA, a propagator developed by Politecnico di Milano [14]. COMETA is a probabilistic long-term debris environment propagator that, in its current implementation, estimates the future evolution of the Low Earth Orbit (LEO) region under the influence of sources—such as launches, satellite explosions, and fragment-intact object collisions—as well as sinks, primarily Post-Mission Disposal (PMD). The model distinguishes between fragments and intact objects. Fragments are represented using a density-based approach and are propagated in time by solving the continuity equation along specific trajectories. The evolution of their semi-major axis and eccentricity is derived from the King-Hele equations [15]. Intact objects, on the other hand, are individually propagated and categorized as payloads, rocket bodies, and, theoretically, constellations—though the latter are not considered in this study, as they are not part of the launch models. The model divides the space into bins based on all orbital parameters, as well as the area-to-mass ratio. Only atmospheric drag is considered as a perturbation, as the analysis focuses on LEO (200–2000 km).

8.1. The distribution of the launched objects

To propagate the evolution of the entire space debris environment not only the number of objects is important but also the orbital characteristics. As mentioned, this analysis only focuses on LEO. Therefore, the distribution is only build based on LEO objects. The probability of the object being in LEO is determined to be 80% and the

number of objects launched each year is adjusted accordingly. Then the probability of each object category in LEO is determined based on historical data between the years 2017 and 2022.

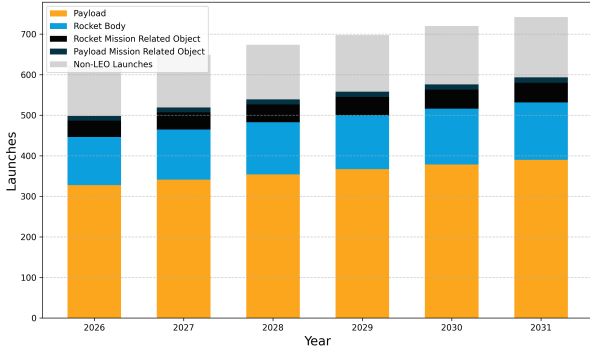


Figure 8. The division of the future launches on the example of the ARIMA forecast. 80% of objects are determined to be in LEO and of these remaining ones they are split in their respective object categories.

Then for the each category in LEO, a 3-dimensional binned distribution of the semi-major axis, the eccentricity and the inclination is built. From this distribution the orbital parameters are randomly drawn for each year. In the propagation with COMETA (see section 8.2) only payload objects are considered. Since the majority of objects are payloads and the focus of this paper is a sensitivity analysis and not to determine the true total number of objects, this adjustment has been made to save for computational time. Therefore, in the following only the payload distribution is discussed further. For better visibility only the 2D projection of the inclination vs. the semi-major axis (Fig. 9) and the 2D projection of semi-major axis vs. eccentricity (Fig. 10) are plotted here. For all dimensions the bin size is determined to be $\sqrt{N} = 36$, with $N=1306$ the number of payload objects between 2017 and 2022.

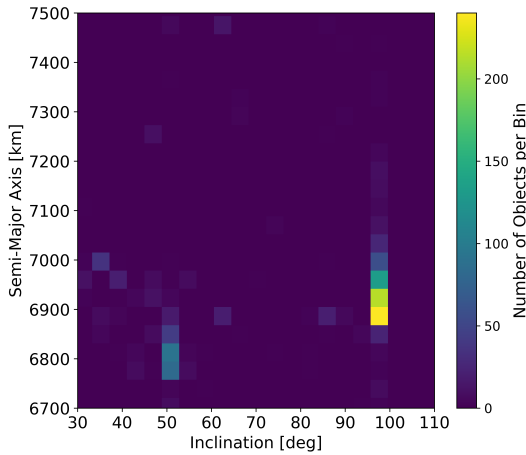


Figure 9. Inclination vs. semi-major axis distribution of payloads in LEO

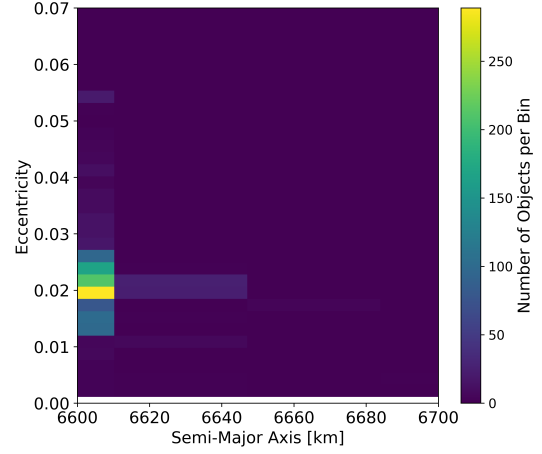


Figure 10. Semi-major axis vs. eccentricity distribution of payloads in LEO

The distribution in inclination vs. semi-major axis shows a clear cluster around an inclination of $97 - 100^\circ$, which is a common inclination for Sun-Synchronous Orbits (SSO). These are often used for Earth observation. Furthermore, around $50 - 55^\circ$ there is another cluster. This follows an ISS-like orbit. The eccentricity has a clear predominance around 0: the majority of LEO satellites are in a circular orbit.

8.2. Evolution with COMETA

At each timestep, the model incorporates newly launched satellites, distributed by launch altitude, while removing those that reach the end of their operational life. PMD is modeled assuming a deorbit time of 25 years for elliptical orbits. The operational lifetime of satellites is set to eight years—shorter than IADC’s 25-year PMD guideline [16] but more representative of the actual lifespan of LEO satellites. A PMD compliance rate of 90% is assumed, reflecting an optimistic scenario. Satellites are considered capable of maintaining their orbits until the end of their operational life. Beyond PMD, only satellite-fragment collisions are estimated by selecting representative targets within each semi-major axis and inclination bin and calculating their collision probability based on the local fragment cloud density. Fragment generation follows NASA’s Standard Breakup Model [17], widely used in other evolutionary models. The explosion probability of each intact object is determined based on historical fragmentation event data. The active debris removal is not included in these simulations. The simulation spans 100 years, starting in 2022, with population data—including launch years, orbital parameters, area, and mass—taken from the ESA’s DISCOS database [10]. The model has been tested and is considered reliable. However, due to the exclusion of a significant portion of the current in-orbit population (more than 50% being only Starlink), the predicted number of collisions and generated fragments is lower than the ones that can be found in [14].

The results of the simulation illustrate how modifying the launch model, while keeping other source and sink mechanisms constant, leads to significantly different outcomes. Despite these variations, all scenarios exhibit a general increasing trend in the total number of objects in orbit. In Fig. 11, the raw data related to fragment evolution are plotted.

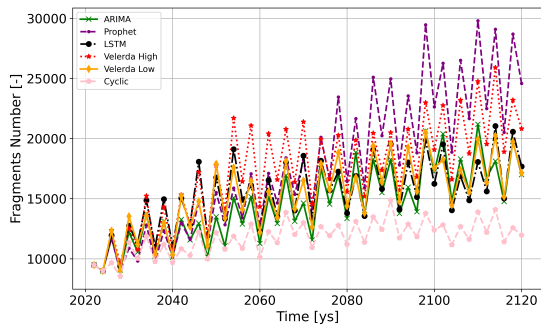


Figure 11. The evolution of fragments for a time span of 100 years with COMETA.

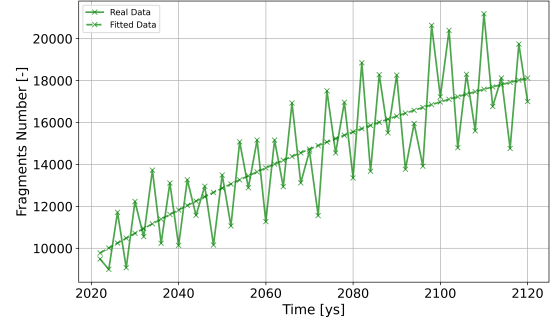


Figure 12. Comparison of real vs. fitted data of the fragments for a time span of 100 years for the ARIMA model

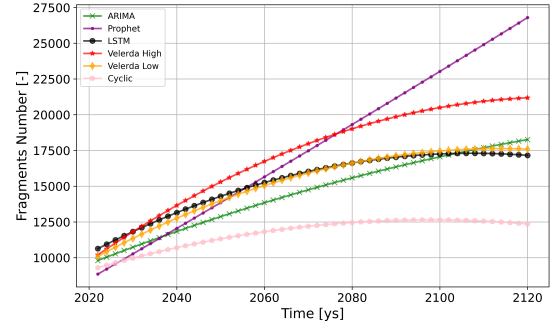


Figure 13. The fitted data of the fragments for a time span of 100 years for all the models

Due to the chosen time step (two years) and the distribution of objects in orbital parameters across different models, some exhibit significant jumps in the number of fragments between time steps, in contrast to the results presented in [18]. Since only one simulation was performed for each model, preventing the possibility of averaging multiple runs for a smoother result, a curve fitting has been applied, as shown in Fig. 12 for the ARIMA model. This adjustment is necessary because the absolute values of these results should not be interpreted as precise (for example, due to the exclusion of satellite constellations). Instead, they serve as a sensitivity analysis of different launch traffic scenarios, making the overall trends more discernible in Fig. 13. As shown in Fig. 14, the Prophet model predicts the most significant growth, with a steep rise and a peak exceeding 40,000 objects by 2120. This suggests a potentially critical escalation in debris accumulation, in stark contrast to the cyclic model, which stabilizes around 20,000 objects in this simulation. The ARIMA, LSTM, and Velarda models present a more moderate increase, with the Velarda High Rate scenario leading to faster debris accumulation compared to the Velarda Low alternative. The cyclic model, which replicates past launch activity, results in the slowest growth of fragments, even when compared to models like Velarda Low Rate, LSTM, and ARIMA.

All four of these models show similar trends in the absolute number of intact objects; however, the increase in the fragment cloud is over 50% for the Velarda, LSTM,

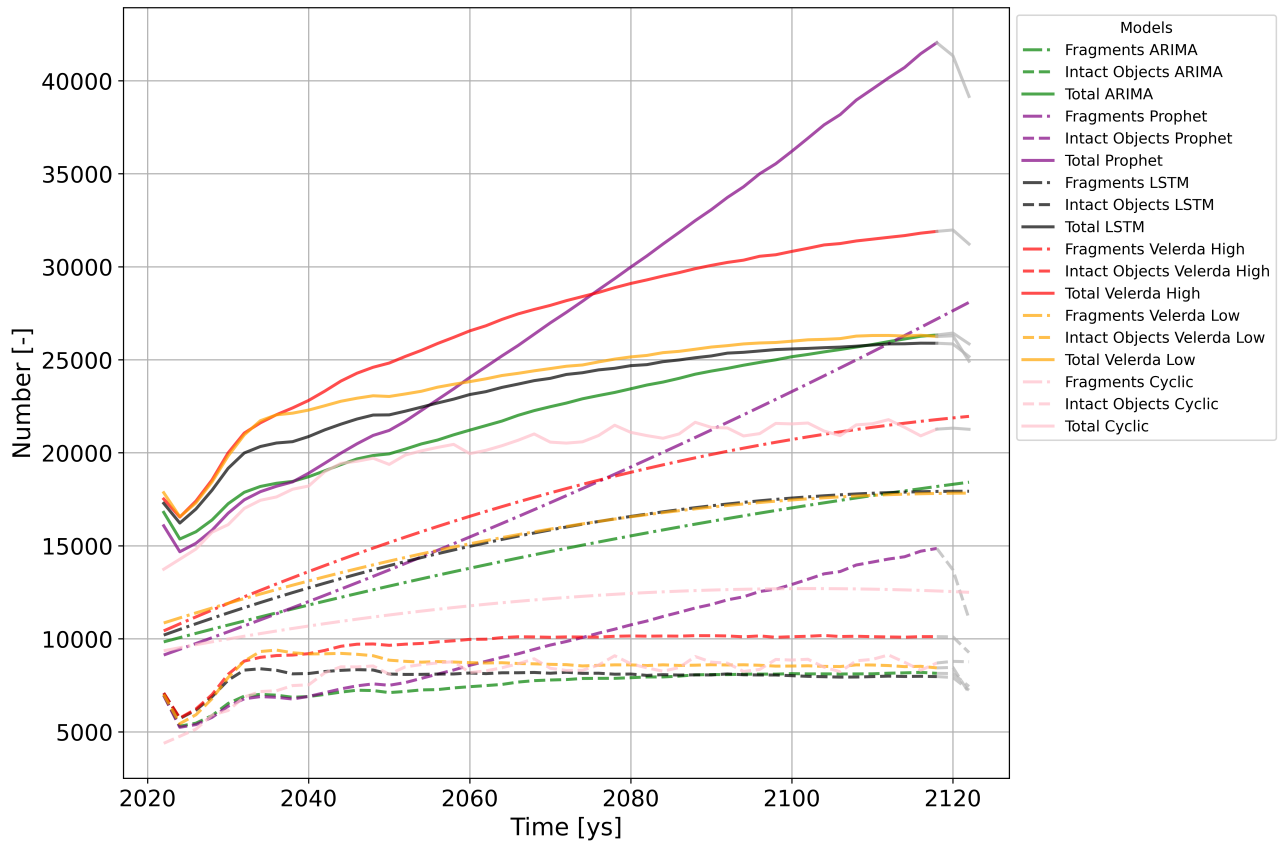


Figure 14. Sensitivity analysis for the evolution of the number of objects, fragments and total population for a time span of 100 years with COMETA.

and ARIMA models, compared to only 30% for the cyclic model. This discrepancy suggests that further analysis is needed to determine how the differences in launch models contribute to the varying fragmentation rates, given that all other conditions remain equal. Regarding intact objects, the trends for all models reflect the characteristics of their respective launch models. In Fig. 14, the final two simulation steps have been disregarded due to an observed sudden drop, which is likely caused by a bug in the code rather than a real physical phenomenon. Although these data points are included in the plot, they should not be considered representative of actual orbital behavior. Moreover, a key limitation of the cyclic model is the evident oscillation in the number of objects over time. This fluctuation is directly linked to variations in past launch rates, which have increased dramatically from approximately 50 to over 200 launches per year in LEO, even excluding large satellite constellations. Despite limiting the repeated launch cycle to just five years, the model still produces traffic variations that lack a clear trend, making it an unrealistic representation of real-world conditions. In contrast, the other models offer a more representative outlook, with some exhibiting an optimistic steady-state behavior, while others suggest a pessimistic scenario of continuous and uncontrolled debris growth. These findings highlight the critical role of launch patterns in the long-term sustainability of the orbital environment and

emphasize the need for mitigation strategies to prevent an unsustainable increase in space debris.

9. OUTLOOK AND CONCLUSION

In this work different methods for forecasting the launch traffic have been investigated. The here presented launch models range widely in the complexity behind them. Going from a simple repetition of the last years, to a curve fit, to statistical models and finally, a machine learning model. While their intricacy varies, they all arrive at very similar final launches for the time span simulated (see Fig. 7). Most of them show a steady upward trend with a saturation point. There are two main outliers: The Prophet model and the cyclic model. The Prophet model keeps on growing and exceeds the other models after roughly 50 years. The cyclic model instead is the only model which simulates also a downward trend for future launches. While currently the number of launches is rising drastically, this rise cannot go on forever. Therefore, a model which also simulates a drop in launches is realistic, especially looking at the historical data. As seen in Fig. 4 the historical data shows a clear seasonality. In the subsequent work this seasonality should be further investigated and other data

such as economic revenue or orbital parameters could be correlated to launch traffic. With the availability of more data, the use of more complex models such as LSTM could yield a real benefit. The LSTM model is suited to help in finding the cross-correlation between the multiple datasets.

Furthermore, a sensitivity analysis using the COMETA software has been performed. These results should not be taken as representative of the future number of objects, but show the definite influence the launch traffic has on the population as a whole. The number of objects, and especially the number of fragments, shows trends that closely follow the launch projections, emphasizing the direct correlation between launch activity and long-term debris accumulation. The fragmentation growth rate differs significantly between models, with more optimistic launch scenarios leading to slower debris proliferation, while high-growth scenarios result in an escalating number of fragments. This illustrates the importance of long-term launch planning and debris mitigation strategies to prevent uncontrolled orbital debris buildup. This work has served as a Proof of Concept of using the presented launch models in conjunction with a space debris environment propagator. In future work this link will be improved and more simulations will be run, delivering statistically relevant results.

ACKNOWLEDGMENTS

The research received funding from the European Research Council (ERC) under the European Union's Horizon Europe research and innovation program as part of the GREEN SPECIES project (Grant agreement No - 101089265).

REFERENCES

1. Somma, G.L., Lewis, H.G. & Colombo, C. (2019). Sensitivity analysis of launch activities in Low Earth Orbit. *Acta Astronautica*, **158**, 129–139. <https://doi.org/10.1016/j.actaastro.2018.05.043>.
2. Krisko, P.H., Johnson, N.L. & Opiela, J.N. (2001). EVOLVE 4.0 orbital debris mitigation studies. *Advances in Space Research*, **28**(9), 1385–1390.
3. Lewis, H.G. (2020). Understanding long-term orbital debris population dynamics. *Journal of Space Safety Engineering*, **7**(3), 164–170.
4. Liou, J-C., Johnson, N.L. & Hill, N.M. (2010). Controlling the growth of future LEO debris populations with active debris removal. *Acta Astronautica*, **66**(5-6), 648–653.
5. Dolado-Perez, J.C., Revelin, B. & Di-Costanzo, R. (2015). Sensitivity analysis of the long-term evolution of the space debris population in LEO. *Journal of Space Safety Engineering*, **2**(1), 12–22.
6. Montgomery, D.C., Jennings, C.L. & Kulahci, M. (2015). *Introduction to time series analysis and forecasting*. John Wiley and Sons.
7. Almasarweh, M. & Alwadi, S. (2018). ARIMA model in predicting banking stock market data. *Modern Applied Science*, **12**(11), 309. <https://doi.org/10.5539/mas.v12n11p309>.
8. Taylor, S. & Letham, B. (2017). Forecasting at scale. *PeerJ Preprints*. 10.7287/peerj.preprints.3190v2.
9. Hochreiter, S. & Schmidhuber, J. (1997). Long Short-Term Memory. *Neural Computation*, **9**(8), 1735–1780. <http://dx.doi.org/10.1162/neco.1997.9.8.1735>.
10. Flohrer, T., Lemmens, S., Bastida Virgili, B., Krag, H., Klinkrad, H., Parrilla, E., Sanchez, N., Oliveira, J. & Pina, F. (2013). DISCOS-current status and future developments. *Proceedings of the 6th European Conference on Space Debris*, **723**, 38–44.
11. Dickey, D.A. & Fuller, W.A. (1979). Distribution of the Estimators for Autoregressive Time Series With a Unit Root. *Journal of the American Statistical Association*, **74**(366), 427–431. <https://doi.org/10.2307/2286348>.
12. Speagle, J.S. (2020). A Conceptual Introduction to Markov Chain Monte Carlo Methods. *arXiv*, stat.OT. <https://arxiv.org/abs/1909.12313>.
13. Velerda Escobar, J.C. (2022). Continuum approach for the modelling of debris population and launch traffic in Low Earth Orbit. Master's Thesis, Politecnico di Milano, School of Industrial and Information Engineering, Department of Aerospace Science and Technology. Supervisor: Colombo, C. Co-supervisor: Giudici, L.
14. Giudici, L. (2024). Space debris environment analysis with continuum mechanics. PhD thesis, Politecnico di Milano. Supervisors: Colombo, C. & Letizia, F.
15. King-Hele, D.G. (1964). *Theory of satellite orbits in an atmosphere*. Butterworths Mathematical Text.
16. IADC Steering Group & Working Group 4. (2025). IADC Space Debris Mitigation Guidelines. Inter-Agency Space Debris Coordination Committee.
17. Krisko, P.H. (2011). Proper implementation of the 1998 NASA breakup model. *Orbital Debris Quarterly News*, **15**(4), 1–10.
18. Giudici, L., Colombo, C., Horstmann, A., Letizia, F. & Lemmens, S. (2024). Density-based evolutionary model of the space debris environment in low-Earth orbit. *Acta Astronautica*, **219**, 115–127. <https://doi.org/10.1016/j.actaastro.2024.03.008>.